Modelling a stellar core

Project 1, AST3310
Spring 2019

Jowita Borowska

1 Introduction

The project is built upon the concepts of energy production and its transport in the central parts of a star. Main goal is to model a star that has a core ($L < 0.995L_0$) reaching out to at least 10% of the initial radius, as well as luminosity, mass and radius that all converge within the range of $0 - 5\%$ of their initial values. In order to do that, some assumptions about the studied gas have been made. First of all, mass fractions of each atomic species are known, they are independent of radius and do not change in time. Furthermore, we assume fully ionized, ideal gas and energy produced entirely as a result of Proton-Proton chain reactions. We are about to integrate our way toward the center of the star, varying values of some initial parameters (radius, density, temperature and pressure) with the purpose of finding the best-fit ones, fulfilling the mentioned goals.

2 Method

2.1 Equations governing the core structure

The computer program that has been written (using Python) solves numerically equations governing the internal structure of the radiative core of a star. Mass, m, is used as the independent variable of the partial differential equations. These are:

$$\frac{\partial r}{\partial m} = \frac{1}{4\pi r^2 \rho} \tag{1}$$

$$\frac{\partial P}{\partial m} = -\frac{Gm}{4\pi r^2} \tag{2}$$

$$\frac{\partial L}{\partial m} = \varepsilon \tag{3}$$

$$\frac{\partial T}{\partial m} = -\frac{3\kappa L}{256\pi^2 \sigma r^4 T^3} \tag{4}$$

The first differential equation (1) comes from the expression for mass within a radius, $m(r)$. The second one (2) comes from the assumption of hydrostatic equilibrium. The third one (3) - from the definitions of luminosity, L, and energy generation per unit mass, ε. Whereas (4) is a solution to the radiative diffusion equation (with no conduction nor convection).
In addition, we have:

$$P = P_G + P_{rad} \Rightarrow \rho(P, T) \tag{5}$$

$$\varepsilon = \sum Q_{ik} r_{ik} \tag{6}$$

Equation (6) defines the full energy generation per unit mass $\left[\frac{\mathrm{J}}{\mathrm{kgs}}\right]$ as the sum of reaction rates per unit mass, r_{ik}, and energies, Q_{ik}, produced through PP chains reactions. Equation (5) gives the pressure as the sum of radiative pressure contribution, $\mathrm{P_{rad}}$, and gas pressure, $\mathrm{P_G}$. The radiative pressure is only temperature-dependent and given by

$$P_{rad} = \frac{a}{3} T^4 = \frac{4\sigma}{3c} T^4, \tag{7}$$

where σ is Stefan-Boltzmann constant and c is the speed of light.
The gas pressure can be found from the equation of state for an ideal gas (as it is assumed to be):

$$P_G V = N k_B T = \frac{m}{\mu m_u} k_B T = \frac{\rho V}{\mu m_u} k_B T \Rightarrow P_G = \frac{\rho k_B T}{\mu m_u}, \tag{8}$$

where N is the number of particles within a volume V (equal to the mass inside that volume, m, divided by the average atomic weight of the particles, μ, and the atomic mass unit, m_u) and k_B is Boltzmann constant. The expression for density, we are looking for, can then be derived from the equation above as

$$\rho(P, T) = P_G \frac{\mu m_u}{k_B T} = (P - P_{rad}) \frac{\mu m_u}{k_B T} = \left(P - \frac{4\sigma T^4}{3c} \right) \frac{\mu m_u}{k_B T}. \tag{9}$$

The only unknown variable is now the average molecular weight of the particles (in atomic mass units), μ. It is defined as dimensionless quantity:

$$\mu = \frac{\overline{m}}{m_u} = \frac{\frac{\rho}{n}}{m_u},$$

where we have used that average mass per particle, $\overline{m}$, is equal to the mass density, ρ, divided by number density, n (total number of particles per unit volume). In order to determine μ, the average mass per particle has to be found by adding all particles in the gas. For n_e being the number density of electrons in the gas and n_i - number density of atoms of type i (with corresponding mass $m_i = A_i m_u$, where A_i is mass number), we have:

$$\overline{m} = \frac{\sum_i n_i m_i + n_e m_e}{\sum_i n_i + n_e} \approx \frac{\sum_i n_i m_i}{\sum_i n_i + n_e} \approx \frac{\sum_i n_i A_i m_u}{\sum_i n_i + n_e},$$

so that:

$$\mu = \frac{\overline{m}}{m_u} = \frac{\sum_i n_i A_i}{\sum_i n_i + n_e}.$$

In general, the number density of electrons depends of ionization state of the gas. As we have assumed fully ionized gas ($n_e \to \sum_i n_i Z_i$, where Z_i is atomic number), we get:

$$\mu = \frac{\sum_i n_i A_i}{\sum_i n_i (1 + Z_i)}.$$

Furthermore, the number densities, n_i, can be found from already mentioned mass fractions of the elements in the gas. We have $X = 0.7$ for hydrogen, $Y = 0.29$ for helium and $Z = 0.01$ for *metals* (all other elements combined), so that the number densities for hydrogen and helium are:

$$n_H = \frac{\rho}{m_u}\frac{X}{A_H} = \frac{\rho X}{1 m_u}, \qquad n_{He} = \frac{\rho}{m_u}\frac{Y}{A_{He}} = \frac{\rho Y}{4 m_u},$$

and expressions above together with the approximation for contribution from *metals*, $(1 + Z_m)/A_m \approx 1/2$, give:

$$\mu = \left[\frac{X}{A_H}(1 + Z_H) + \frac{Y}{A_{He}}(1 + Z_{He}) + \frac{Z}{A_m}(1 + Zm)\right]^{-1} \approx \left[2X + \frac{3Y}{4} + \frac{Z}{2}\right]^{-1},$$

where $X + Y + Z = 1$ has been used. We can now calculate that $\mu \approx 0.62$. (Remark: Y is the fractional abundance by weigth for a mixture of stable helium isotopes, so we could include $Y_3 = 10^{-10}$ for ^{3}He in the sum and use $Y - Y_3$ for ^{4}He, but this would not make a significant difference for the final value of μ).

2.2 Numerical implementation

The start point parameters are in agreement with the bottom of the solar convection zone ($R_0 = 0.72 R_\odot$, $\rho_0 = 7200 \frac{\text{kg}}{\text{m}^3} \approx 5.1 \overline{\rho}_\odot$, $T = 5.7$MK), initial luminosity is equal to the luminosity of the Sun, $L_0 = L_\odot$, and the mass contained within the initial radius is $M_0 = 0.8 M_\odot$. Initial value of the pressure is calculated by a function, as the sum $\mathrm{P} = \mathrm{P_G} + \mathrm{P_{rad}}$, accordingly to equations (7)&(8). Initial value of ε (and every subsequent one) is computed by the function taking current temperature and density values as input and returning the energy generation. The energy produced through PP fusion chains depends on the rate of each individual step and the availability of elements involved in these reactions. This is restricted by various if-tests (see the code for details).

All the differential equations (in the exact same order: 1-4) are implemented into the program and solved numerically using Euler's method. The values of opacity, κ, appearing in the equation (4), are being read from the file for each step (taking temperature and density as input), linear 2D interpolation is performed in case when exact values are not found in the table (and extrapolation with warning for values outside the bounds of the table). Thereafter, next density is computed by a function consistent with formula (9), followed by calculation of next ε with use of the new temperature and density.

There are two possibilities of advancing the computations in the program - either with a fixed steplength, Δm, or with the dynamic steplength. The latter is implemented as described in *variablesteplength.pdf* and changes its value dependent on the current magnitude of the variable we are stepping forward. The allowed fraction of change, p, has been properly adjusted throughout the process of finding the best model (more about that in the *Discussion* section).

Tests of the functionality and correct implementation of the code were performed for the available *sanity checks* and they all seem to be in agreement with the results produced by the program.

3 Results

3.1 Initial parameters - tests

Several experiments have been conducted in order to investigate how the behaviour of radius, density, temperature, luminosity and pressure changes with variation of initial parameters. Throughout the whole process, the initial values of luminosity ($L_0 = L_\odot$) and mass ($M_0 = 0.8M_\odot$) are kept the same, but we vary separately R_0, T_0 and ρ_0. As the initial value of pressure, P_0, is calculated by a function taking T_0 and ρ_0 as input (because we hold to the ideal gas assumption), changes in the initial temperature or density have also an impact on the initial value of pressure.

Many different tests have been performed, varying initial values up to the factor of 5. However, we choose to include the ones showing explicit tendencies (what happens if a given parameter has lower or higher initial value), but being simultaneously possible to demonstrate on the same scale in one plot for comparison.

- Test of the initial values of **radius**, R_0: $0.72R_\odot$, $0.6R_\odot$, $1.2R_\odot$.
  Other parameters: $T_0 = 5.7$ MK, $\rho_0 = 7200\frac{\text{kg}}{\text{m}^3}$, $P_0 = 5.54 \cdot 10^{14}$Pa.

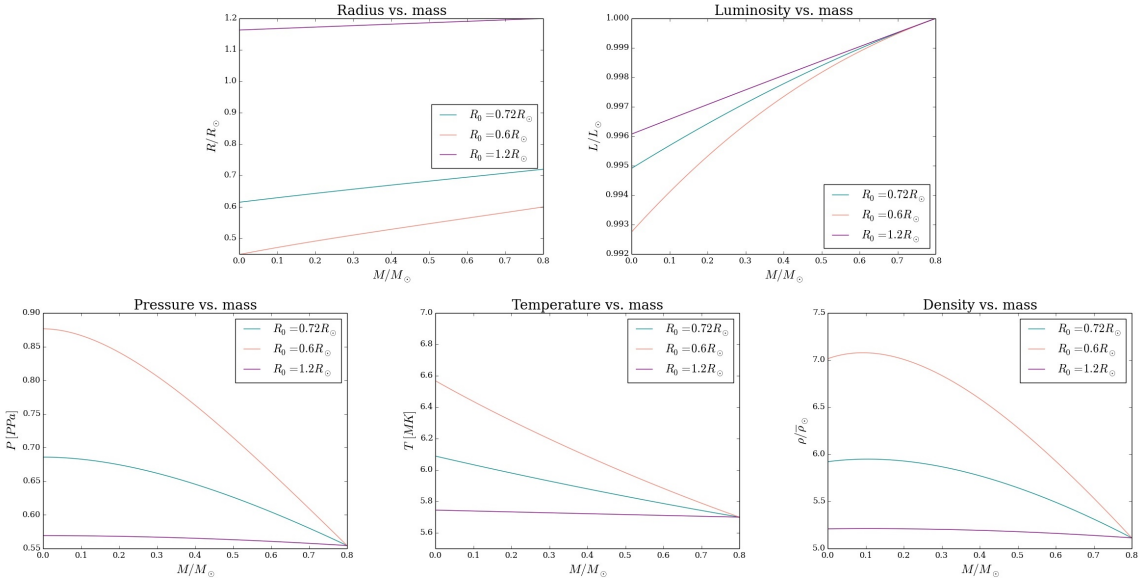

Figure 1: Test of the initial values of radius for R_0 equal: $0.72R_\odot$, $0.6R_\odot$ and $1.2R_\odot$. Plots show the behaviour of radius, luminosity, pressure, temperature and density as the mass within the radius, $M(R)$, changes. Luminosity, mass, radius and density are scaled with corresponding values for the Sun (density with the average density of the Sun, $\overline{\rho}_\odot$). Pressure is given in PPa (10^{15}Pa).

Figure 1. shows the exemplary impact of initial radius variations on other parameters. From all the performed experiments we can clearly see that the smaller value of R_0 leads to: faster decreasing radius (slightly bigger slope of $R(M)$), more rapidly decreasing luminosity, higher final pressure, temperature and density. Increasing the initial value of R_0 leads to opposite conclusions.

- Test of the initial values of **density**, ρ_0: 7200 $\frac{\text{kg}}{\text{m}^3}$, 1500 $\frac{\text{kg}}{\text{m}^3}$ and 11000$\frac{\text{kg}}{\text{m}^3}$.
  Other parameters: P_0, consecutively: $5.54 \cdot 10^{14}$Pa, $1.16 \cdot 10^{14}$Pa and $8.47 \cdot 10^{14}$Pa, $T_0 = 5.7$ MK, $R_0 = 0.72 R_\odot$.

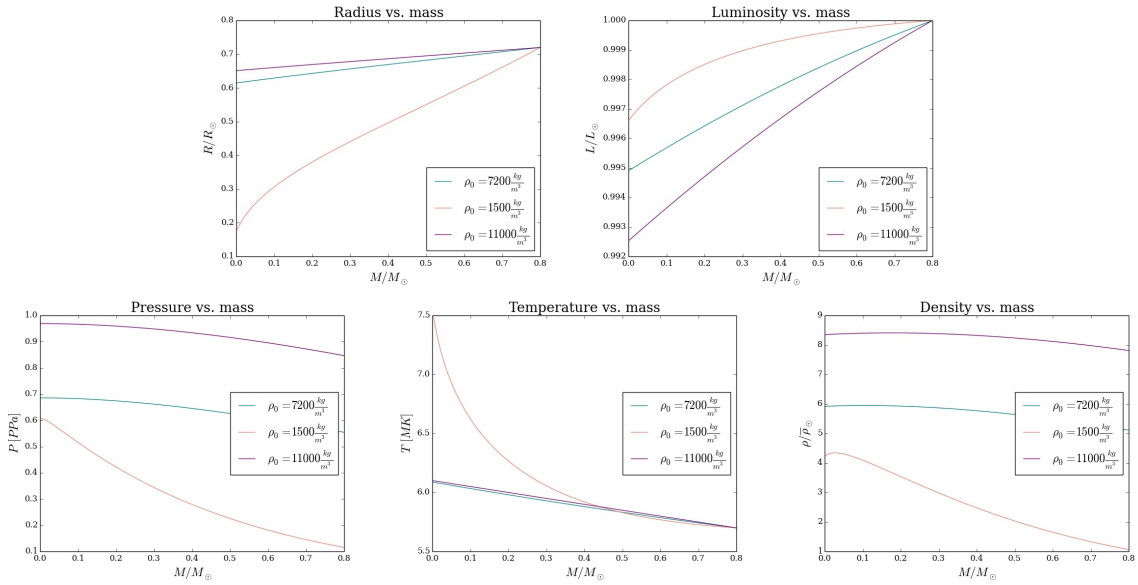

Figure 2: Test of the initial values of density for ρ_0 equal: 7200 $\frac{\text{kg}}{\text{m}^3}$, 1500 $\frac{\text{kg}}{\text{m}^3}$ and 11000$\frac{\text{kg}}{\text{m}^3}$. Plots show the behaviour of radius, luminosity, pressure, temperature and density as the mass within the radius, $M(R)$, changes. Luminosity, mass, radius and density are scaled with corresponding values for the Sun (density with the average density of the Sun, $\overline{\rho}_\odot$). Pressure is given in PPa (10^{15}Pa).

Figure 2. shows the exemplary impact of initial density variations on other parameters. It is easy to deduct that lower initial density gives smaller initial pressure. Furthermore, tests indicate that smaller ρ_0 leads also to significantly more rapidly decreasing radius, slightly bigger final luminosity, as well as faster rise of pressure, temperature and density. A little bit higher ρ_0 naturally produces opposite results, but the changes are not so explicit in this case, as can be seen on figure 2.

- Test of the initial values of **temperature**, T_0: 5.7 MK, 4.5 MK and 8.0 MK. Other parameters: P_0, consecutively: $5.54 \cdot 10^{14}$Pa, $4.38 \cdot 10^{14}$Pa and $7.79 \cdot 10^{14}$Pa, $R_0 = 0.72 R_\odot$, $\rho_0 = 7200 \frac{\text{kg}}{\text{m}^3}$.

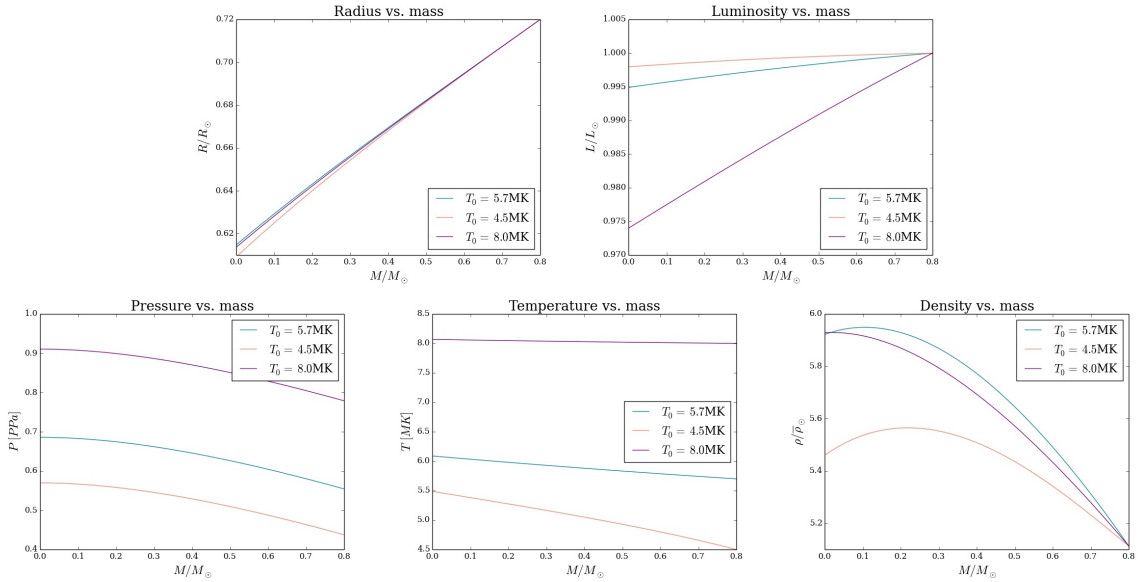

Figure 3: Test of the initial values of temperature for T_0 equal: 5.7 MK, 4.5 MK and 8.0MK. Plots show the behaviour of radius, luminosity, pressure, temperature and density as the mass within the radius, $M(R)$, changes. Luminosity, mass, radius and density are scaled with corresponding values for the Sun (density with the average density of the Sun, $\overline{\rho}_\odot$). Pressure is given in PPa (10^{15}Pa).

Figure 3. shows the exemplary impact of initial temperature variations on other parameters. Again, it is clear that higher initial temperature gives higher P_0. Moreover, the smaller temperature the faster decrease of radius (but these changes are not very siginificant). Luminosity drops faster for bigger T_0. The temperature slope is a bit bigger for lower values of T_0 and plots of pressure are almost parallel, while density plots indicate rather small variations between final density values (all lie within 0.5 $\overline{\rho}_\odot$).

3.2 Best model

The goal is to create a model where radius, mass and luminosity all converge to zero or at least within the range $0 - 5\%$ of their initial values. Considering all the information acquired throughout experiments with various initial values, we start by lowering ρ_0 in order to decrease radius more rapidly while the mass is progressing toward zero. This results in fast increase of density while we move toward the center of the star, as we have seen before. Furthermore, lower value of initial radius gives luminosity that decreases much faster, so the next action has been making the star smaller. Rising the initial value of temperature gives simiar results. Therafter, series of adjustments has been made, introducing the small changes in T_0, ρ_0 and R_0, applying the knowledge gathered through experminets, as well as keeping track of the final values and the goal.

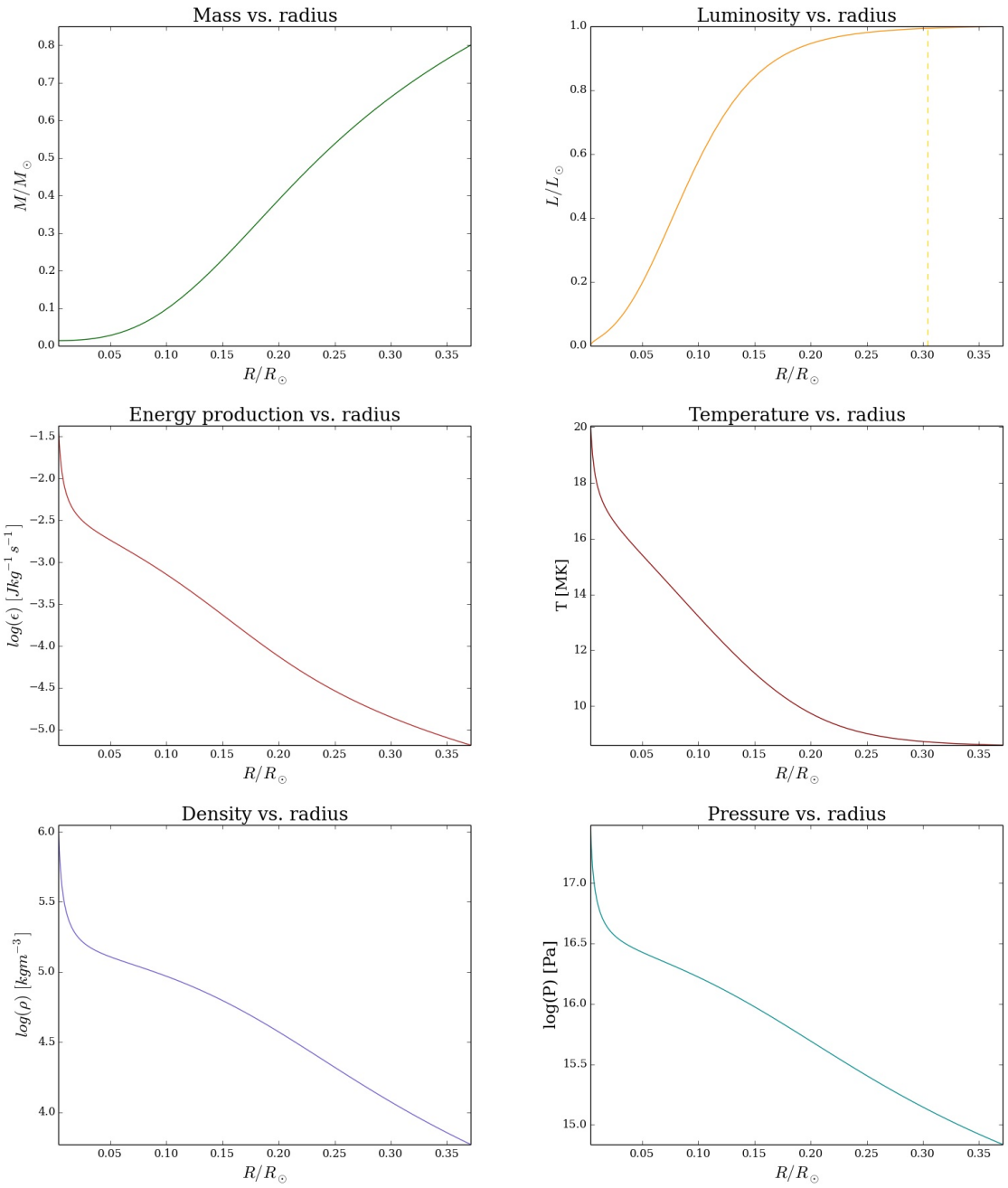

Figure 4: Best model: $R_0 = 0.3711 R_\odot$, $\rho_0 = 5900\ \frac{\text{kg}}{\text{m}^3}$, $T_0 = 8.6$ MK, $P_0 = 6,87 \cdot 10^{14}$Pa. Plots show the behaviour of mass, luminosity, pressure, temperature, density and energy production as the radius changes. Luminosity, mass and radius are scaled with corresponding values for the Sun. Pressure, density and energy production are shown with logarithmic axes. Dashed vertical line on the luminosity plot marks the beginning of core ($L < 0.995 L_0$).

The best model has $M_0 = 0.8M_\odot$, $L_0 = L_\odot$ (as these were held fixed throughout the whole project), $R_0 = 0.3711R_\odot$, $\rho_0 = 5900\ \frac{\text{kg}}{\text{m}^3}$, $T_0 = 8.6$ MK, $P_0 = 6,87 \cdot 10^{14}$Pa. Even though the extrapolation of opacity values, κ, was possible (and encountered throughout the process of adjusting parameters to get the best model), we were able to avoid extrapolation, staying in the bounds of the table throughout all ρ and T values. The final mass is equal to 1.72% of M_0, final radius - 1.06% of R_0 and final luminosity - 0.16% of L_0. Temperature rises up to 20.05 MK at the center, pressure to $3.02 \cdot 10^{17}$Pa and density to $1.12 \cdot 10^6 \frac{\text{kg}}{\text{m}^3}$. Energy generation per unit mass increases from the initial value equal $\varepsilon_0 = 6.55 \cdot 10^{-6}\ \frac{\text{J}}{\text{kgs}}$ to 0.0427 $\frac{\text{J}}{\text{kgs}}$ at the center. The core reaches out to 81.94% of R_0 ($L < 0.995L_0$ in this area).

Figure 4 shows how mass within the radius, luminosity, pressure, temperature, density and energy generation per unit mass change with the radius (cross section of the star).

4 Discussion and conclusions

4.1 Analysis of experiments with various initial values

Results of tests with various initial values of R_0, ρ_0, T_0 and P_0 could have been predicted by analysing the set of equations to be solved numerically (equations 1-6 introduced in the *Method* section). We need to keep in mind that the mass progresses toward zero, so Δm is negative.

Equaiton (1) defines the change in radius as the mass changes. We can see that $\frac{\partial R}{\partial M}$ is inversely proportional to the product $R^2\rho$. No wonder that lower ρ_0 results in the more rapid decrease of radius and lower R_0 has the same consequences. The initial values for radius and density could be balanced out here, so that increasing R_0 twice and simultaneously decreasing ρ_0 by a factor of 4 leads to the same radius-slope, $\frac{\partial R}{\partial M}$.

Equation (2) gives the change of pressure $\frac{\partial P}{\partial M}$. It is negative, which means that as the integration advances and mass is decreasing, pressure is increasing. It is also inversely proportional to the R^4. This suggests that smaller R_0 results in rapid increase of pressure, which is in agreement with conducted experiments.

The luminosity-slope, $\frac{\partial L}{\partial M}$, depends on the energy generation per unit mass, ε (see equation 3), which is generally higher for higher temperatures and densities (more reactions occur $\Rightarrow$ more energy is produced in a star). Decrease of luminosity should then be more rapid for higher T_0 and ρ_0, which is indeed confirmed by the tests. T_0 and ρ_0 could be in principle also balanced out here (by increasing one and decreasing another), but energy production is very complex and in general much more complicated to analyse in order to find the clear relation between T and ρ dependence.

Last differential equation (4), relates the change of temperature to the mass-change. Minus sign indicates that T is increasing as the mass is integrated toward zero. The temperature-slope, $\frac{\partial T}{\partial M}$ is inversely proportional to the product R^4T^3, so that smaller R_0 and smaller T_0 result in the more rapid rise of the temperature. Once again, this analysis is in agreement with the data acquired from experiments with initial values. Moreover, keeping the product R^4T^3 constant, would in principle hold the temperature-slope unchanged, but there is also luminosity and κ in the numerator of equation (4), which makes its behaviour more complicated and unpredictable.

Furthermore, we can clearly see (from equations 7 and 8) that the pressure, $P_{rad} + P_G$, has higher value for bigger density and temperature. Increasing ρ_0 and T_0 naturally increases P_0

as well, but as neither T nor ρ appears in the differential equation giving $\frac{\partial R}{\partial M}$ (2), the initial values of these parameters do not have a direct impact on the shape of pressure-slope (so that the pressure plots for slightly different ρ_0 and T_0 are almost parallel). Nevertheless, we need to keep in mind that the set of equations is being solved as a whole, so that when much lower ρ_0 produces rapidly decreasing radius, the temperature rise is also rapid and hence - pressure rise.

All the equations, solved numerically in each iteration of the program, are tightly bound togehter. As the various parameters have an impact on different parts of the model, we always need to look at the set of equations in its entirety and the best way to do that is analysing the numerical solution. Nevertheless, some conclusions about the behaviour of different parameters can be drawn just by analytical analysis, as we have seen in this section.

4.2 Analysis of best model

Following the strategy explained in the previous section, we are able to create a model that fullfils set goals. Convergence point is not exactly zero, but very close - the final mass is equal to 1.72% of M_0, final radius - 1.06% of R_0 and final luminosity - 0.16% of L_0. However, these values are rather large as M_0, R_0 and L_0 are big numbers. Figure 4 shows the evolution of six parameters as a function of radius, being a good model for a cross section of the star. Luminosity rises slowly at the end (looking at the plot in the direction of increasing radius), so that $0 - 81.94\%$ of R_0 makes up the core (area where $L < 0.995L_0$), marked on the plot by a dashed line . We can see that energy generation per unit mass, temperature, density and pressure are increasing toward the center of the star and that increase is more rapid closer to $R \approx 0$. Radius decreses in the similar manner - faster closer to the center. This is in agreement with the analysed equations - the smaller radius, the faster it drops (eq. 1), and also the faster temperature, pressure and hence - density - rises (eq. 2 & 4). Energy production, dependent on the temperature and density, is obviously higher in the central parts of the core as well.

Tendencies in the behaviour of all the considered quantities coud have been predicted to some extent by the closer analysis of equations. This makes our final model consistent with both assumptions and the initially set goals.

4.3 Fixed vs. dynamic steplength

The program solves the set of equations numerically, advancing the computations by a certain change in mass, Δm. In order to not to proceed with calculations when there is "no mass left" to integrate, we cut the program at the point when the mass turns negative.

As already mentioned, there are two possibilities implemented into the program - we can advance integration with a fixed, static steplength or we can swtich on the dynamic steplength, that adjusts its value automatically. The function $R(M)$ has been plotted with the dynamic steplength switched off, for significantly different static steplengths (and very first initial values). However, no major changes between the plots have been observed, so we choose to include only one, for $\Delta m = -10^{-4} M_\odot$ (see figure 5a).

All the tests in the section 3.1 are executed with the dynamic steplength turned on, and the value of possible fractional change equal $p = 0.001$ (see *variablesteplength.pdf* for details). As the values of parameters in the tests are rather big (we have not aimed for convergence to zero yet), this choice of p gives a reasonable amount of datapoints (smaller p would result in a

very big steplength and rapidly advancing integration). We also reach $M = 0$ every time, so that we need to exploit the condition on cutting the program before the mass turns negative.

However, while looking for a best-fit initial values of our final model, the steplength decreases as $R \to 0$ (see figure 5b). This leads to the fact that more datapoints are concentrated toward the end of integration (closer to $R \approx 0$) and it is much harder to get to the point where M is exactly zero. We decide therefore, to cut the program before ΔM gets unreasonably small (smaller than $10^{-6} M_0$). Here, also the value of allowed fractional change has been adjusted to $p = 0.1$, in order to increase the consecutive steplengths.

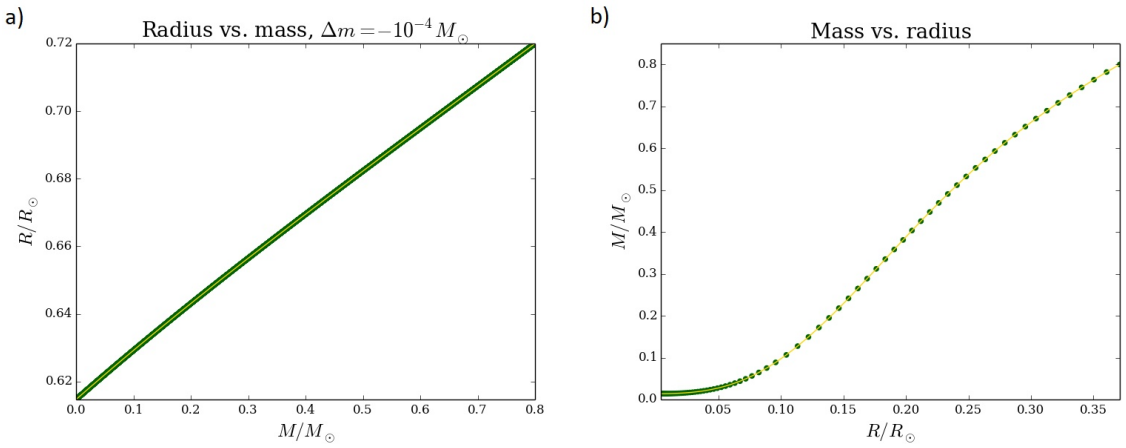

Figure 5: a) Plot of radius as a function of mass, $R(M)$, for the very first initial parameters ($R_0 = 0.72 R_\odot$, $\rho_0 = 7200\ \frac{\text{kg}}{\text{m}^3}$, $T_0 = 5.7$ MK), with the static steplength, $\Delta m = -10^{-4} M_\odot$. b) Plot of mass within radius, $M(R)$, for best model with the actually computed datapoints marked in order to show the variation in the dynamic steplength as the integration advances.